Corrections

IMMUNOLOGY. For the article "Diversity of regulatory $CD4^+$ T cells controlling distinct organ-specific autoimmune diseases," by Marie-Alexandra Alyanakian, Sylvaine You, Diane Damotte, Christine Gouarin, Anne Esling, Corinne Garcia, Séverine Havouis, Lucienne Chatenoud, and Jean-François Bach, which appeared in issue 26, December 23, 2003, of *Proc. Natl. Acad. Sci. USA* (**100,** 15806–15811; first published December 12, 2003; 10.1073/pnas.2636971100), due to a printer's error, the first bar for the cell population $CD25^-CD62L^+$ in Fig. 2 should be open instead of filled. The corrected figure and its legend appear below.

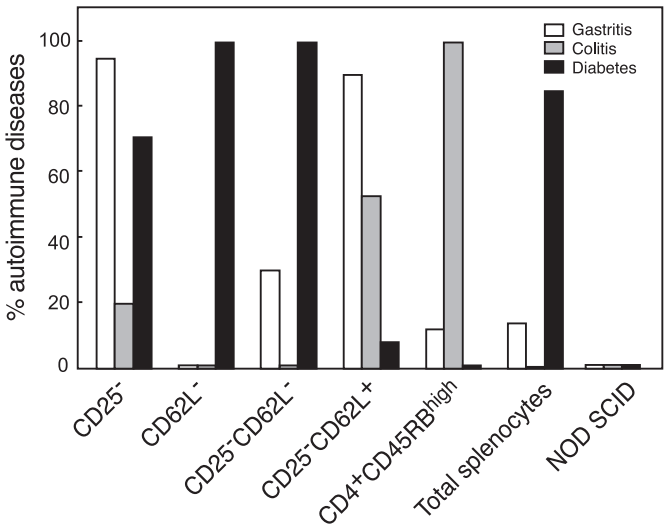

Fig. 2. Gastritis, colitis, and diabetes in NOD SCID mice reconstituted with spleen cells depleted of distinct regulatory T cell subsets. Incidence of overt diabetes and histological gastritis and colitis in a total of 194 NOD SCID mice reconstituted with various T cell subsets is shown. The major finding was that $CD25^-CD62L^+$, $CD4^+CD45RB^{high}$, and $CD4^+CD62L^-$ T cells were unique in their capacity to trigger almost exclusively one disease, namely gastritis, colitis, or diabetes, respectively. Intermediate patterns, both in terms of incidence and severity (see also Table 1), were observed for the other purified subsets.

www.pnas.org/cgi/doi/10.1073/pnas.0400176101

COMMENTARY. For the article "Slow-wave sleep, acetylcholine, and memory consolidation," by Ann E. Power, which appeared in issue 7, February 17, 2004, of *Proc. Natl. Acad. Sci. USA* (**101,** 1795–1796; first published February 9, 2004; 10.1073/pnas.0400237101), the author notes that the phrase "and associated with theta and gamma oscillations" should be omitted from the first sentence of the center column on page 1795. The theta and gamma oscillations are related to information transfer during REM and not to slow-wave sleep. The sentence should have read "Buzsaki (12, 13) has suggested that sharp wave bursts initiated in the hippocampus during SWS may provide the mechanism by which 'quanta' of information may be relayed back to the neocortex during memory consolidation."

www.pnas.org/cgi/doi/10.1073/pnas.0400990101

GENETICS. For the article "Wnk1 kinase deficiency lowers blood pressure in mice: A gene-trap screen to identify potential targets for therapeutic intervention," by Brian P. Zambrowicz, Alejandro Abuin, Ramiro Ramirez-Solis, Lizabeth J. Richter, James Piggott, Hector BeltrandelRio, Eric C. Buxton, Joel Edwards, Rick A. Finch, Carl J. Friddle, Anupma Gupta, Gwenn Hansen, Yi Hu, Wenhu Huang, Crystal Jaing, Billie Wayne Key, Jr., Peter Kipp, Buckley Kohlhauff, Zhi-Qing Ma, Diane Markesich, Robert Payne, David G. Potter, Ny Qian, Joseph Shaw, Jeff Schrick, Zheng-Zheng Shi, Mary Jean Sparks, Isaac Van Sligtenhorst, Peter Vogel, Wade Walke, Nianhua Xu, Qichao Zhu, Christophe Person, and Arthur T. Sands, which appeared in issue 24, November 25, 2003, of *Proc. Natl. Acad. Sci. USA* (**100,** 14109–14114; first published November 10, 2003; 10.1073/pnas.2336103100), the authors note that the software used to generate the original graph depicting historical progression of estimated genome coverage by Omnibank failed to consistently select the earliest Omnibank sequence tag (OST) match to the sentinel gene list. Therefore, the rate of genome coverage is significantly greater in the initial phases of gene trap clone collection than that originally presented in the graph for Fig. 2*B*. The corrected graph accurately illustrates an initial high rate of growth in genome coverage that then slows more significantly in the later stages of clone collection. The conclusions regarding total genomic coverage achieved by this methodology as well as other aspects of the work are unchanged. The corrected figure and its legend appear below.

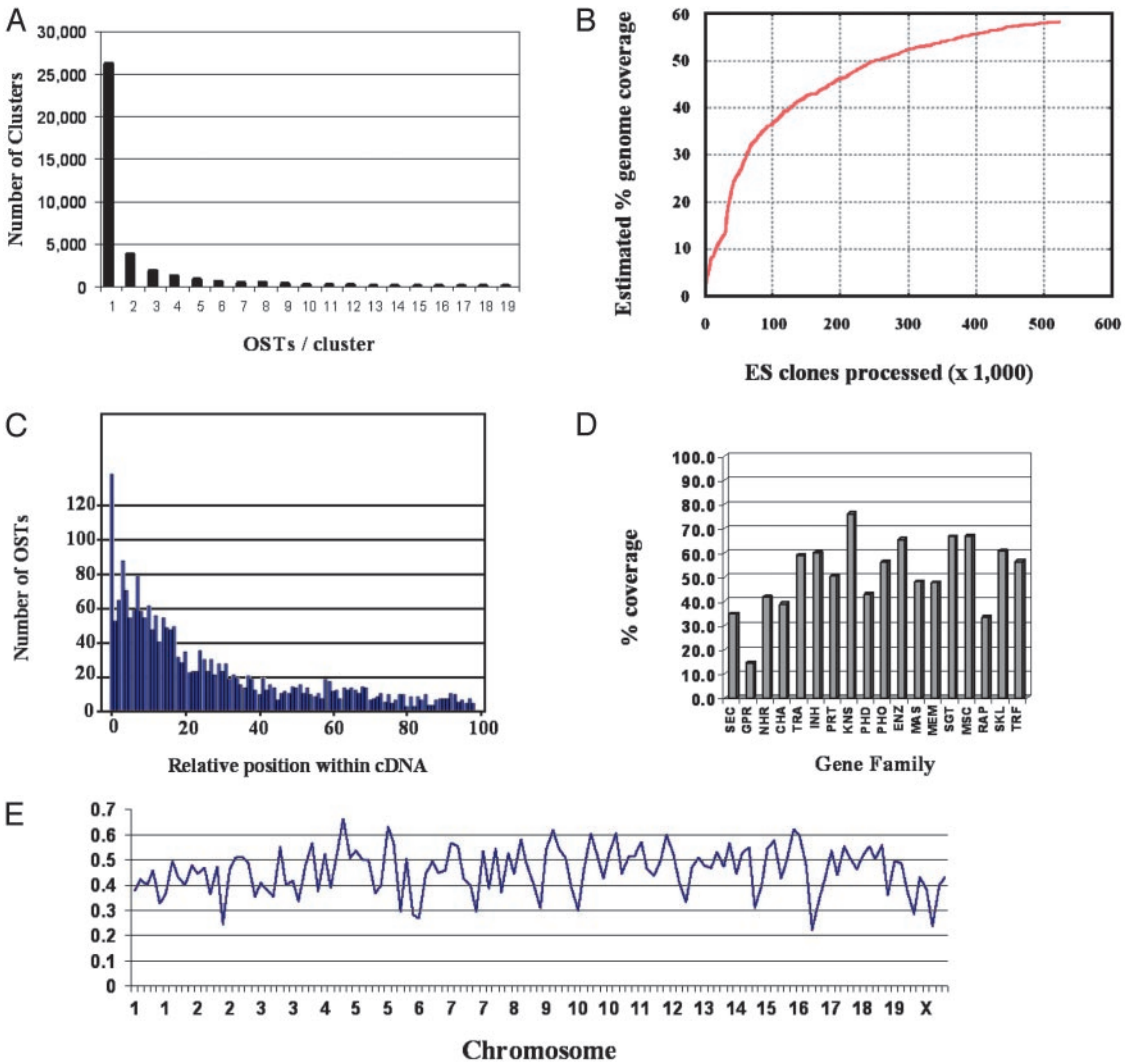

Fig. 2. (*A*) Distribution of OSTs per OmniBank cluster is shown. (*B*) Historic progression of the estimated genome coverage of OmniBank is shown. (*C*) Distribution of OSTs relative to the cDNA sequence within the 2,170 genes analyzed is shown. (*D*) Estimated OmniBank gene coverage by gene family is shown. SEC, secreted; GPR, G protein-coupled receptor; NHR, nuclear hormone receptor; CHA, channel; TRA, transporter; INH, inhibitor; PRT, protease; KNS, kinase; PHD, phosphodiesterase; PHO, phosphatase; ENZ, enzyme; MAS, membrane and secreted; MEM, membrane; SGT, signal transduction; MSC, miscellaneous; RAP, receptor-associated protein; SKL, cytoskeletal; TRF, transcription factor. (*E*) Distribution of OmniBank gene-trap events throughout the mouse genome. Units on the *x* axis represent 20-Mbp genomic intervals. The *y* axis shows the percentage of genes trapped within each 20-Mbp interval. Additional detail on chromosomewide coverage is available in Fig. 6.

www.pnas.org/cgi/doi/10.1073/pnas.0400833101

Diversity of regulatory CD4$^+$ T cells controlling distinct organ-specific autoimmune diseases

Marie-Alexandra Alyanakian*†, Sylvaine You*†, Diane Damotte‡, Christine Gouarin*†, Anne Esling*†, Corinne Garcia†, Séverine Havouis*†, Lucienne Chatenoud*†, and Jean-François Bach*†§

*Institut National de la Santé et de la Recherche Médicale U580, and †Institut Fédératif Necker Enfants Malades, Faculté Necker Enfants Malades, 161 Rue de Sèvres, 75015 Paris, France; and ‡Laboratoire d'Anatomopathologie, Hôpital Georges Pompidou, 20 Rue Leblanc, 75015 Paris France

Communicated by Georges Charpak, European Organization for Nuclear Research, Geneva, Switzerland, October 28, 2003 (received for review August 22, 2003)

Depletion of selected regulatory CD4$^+$ T cell subsets induces the spontaneous onset of various immune or autoimmune disorders. It is not clear, however, whether a given subset, notably CD4$^+$CD25$^+$ regulatory T cells, protects from a wide spectrum of immune disorders, or whether specialized subsets of regulatory T cells control each given disease or group of diseases. We report here, using diabetes prone nonobese diabetic (NOD) mice, that depending on the regulatory T cells that are depleted, i.e., CD25$^+$, CD62L$^+$, or CD45RB^{low}, distinct immune diseases appear after transfer into NOD severe combined immunodeficiency (SCID) recipients. Thus, reconstitution of NOD SCID mice with CD25$^-$ T cells induces major gastritis and late-onset diabetes, but no or mild colitis. Reconstitution with CD62L$^-$ T cells induces fulminant diabetes with no colitis or gastritis. Reconstitution with CD45RB^{high} T cells induces major colitis with wasting disease and no or very moderate gastritis and diabetes. Major differences among the three regulatory T cell subsets are also seen *in vitro*. The bulk of suppressor cells inhibiting the proliferation of CD4$^+$CD25$^-$ T cells in coculture is concentrated within the CD25$^+$ but not the CD62L$^+$ or CD45RB^{low} T cell subsets. Similarly, cytokine production patterns are significantly different for each regulatory T cell subset. Collectively, these data point to the diversity and organ selectivity of regulatory T cells controlling distinct autoimmune diseases whatever the underlying mechanisms.

Experimental evidence has been collected indicating the existence of naturally occurring regulatory CD4$^+$ T cells controlling autoimmunity in various models of experimentally induced lymphopenia (1, 2). Depletion of CD25$^+$ T cells, as obtained after thymectomy at 3 days of age (in BALB/c mice) or by restoring BALB/c nude mice with CD25$^-$ T cells (3) induces the onset of gastritis, thyroiditis, and oophoritis or prostatitis/orchitis, depending on the mouse gender. Reconstitution of BALB/c severe combined immunodeficiency (SCID) mice with CD45RB^{high} T cells (obtained after depletion of CD45RB^{low} T cells) leads to the onset of colitis with severe wasting disease (4). Last, reconstitution of nonobese diabetic (NOD) SCID mice with CD62L$^-$ T cells, obtained after depletion of T cells expressing CD62L (L-selectin), induces rapid onset insulin-dependent diabetes mellitus (5–7). One interpretation of these differences is that, depending on the regulatory T cell subset depleted (CD25$^+$, CD62L$^+$, or CD45RB^{low}), different immune disorders are induced. Another interpretation, favored by several groups, is that differences in mouse strains (BALB/c vs. NOD), experimental conditions (thymectomy, nude, or SCID recipients), and the autoimmune or immune disease examined in each given study could explain the results observed. This latter hypothesis was in keeping with the major attention focused on CD25$^+$ T cells as the central actors in all these models. In addition, as far as colitis is concerned, differences in gut bacterial colonization could have differed according to animal facilities, an important factor because of the well established role of mucosal bacteria in the pathogenesis of inflammatory bowel diseases (8, 9).

We report here that the differences in organ specificity outlined above still hold in well controlled experimental conditions using a single mouse strain (NOD, NOD SCID). These data raise the question of the mechanisms explaining the preferential effect of CD25$^+$, CD62L$^+$, and CD45RB^{low} T cells in the control of immune disorders affecting different organs.

In addition, results from our *in vitro* studies (suppression of CD3 antibody-induced proliferation of CD4$^+$CD25$^-$ T cells and cytokine production) further support the existence of a distinct functional pattern of each of the three regulatory CD4$^+$ T cell subsets.

Materials and Methods

Mice. NOD (K^d, I-A^{g7}, D^b) and NOD SCID mice were bred in our animal facilities under specific pathogen-free conditions. Colorimetric strips were used to monitor glycosuria (Glukotest, Boehringer Mannheim) and fasting glycemia (Haemoglukotest and Reflolux F, Boehringer Mannheim). When needed, diabetic mice were treated with insulin (1–2 units/day).

Flow Cytometry. Biotin, phycoerythrin (PE), FITC, or allophycocyanin (APC)-labeled antibodies to CD62L (MEL-14), CD25 (7D4 or PC61), CD19 (1D3), CD45RB(16A), CD4, CD8, and PE- and APC-labeled streptavidin were from BD Pharmingen. Cells were stained in PBS plus 5% heat-inactivated FCS (Invitrogen) plus 0.01% sodium azide and fixed by using PBS plus 2.5% formaldehyde (Sigma–Aldrich). Control staining was performed by using isotype-matched biotin, FITC, or PE-labeled irrelevant antibodies. CELLQUEST software (Beckton Dickinson) was used for the acquisition and the analysis.

Cell Recovery and Purification. Splenocytes were purified by using magnetic bead-activated cell sorting (MACS, Miltenyi Biotec, Bergisch-Gladbach, Germany), as reported (5, 10). In brief, spleen cells were incubated for 20 min at 4°C in ice with the appropriate concentration of the biotinylated CD4, CD25, CD62L, or CD45RB antibodies. The cells were washed and incubated with streptavidin-coated paramagnetic beads (10 μl/10 $\times$ 10^6 cells) for 15 min at 4°C. After washing, the cells were passed through MS or LS columns within the MACS device. The buffer used throughout the whole procedure was PBS supplemented with 5% FCS. T cell purity was >97%, and recovery ranged from 50% to 70%. For some experiments, cells were purified by using fluorescence-activated cell sorting (FACS, FACSVantage, Becton Dickinson). CD4$^+$ T cells, recovered by negative selection by using a CD4$^+$ T cell isolation kit (MACS), were stained with FITC, phycoerythrin, and allophycocyanine-Sav-conjugated antibodies to CD25, CD62L, or biotinylated antibody to CD45RB. The cells were washed, resuspended in a 2% FCS-containing culture medium deprived of phenol red, and FACS-sorted (purity was ≈98%).

Adoptive Cell Transfer. Recipients were adult 6-wk-old NOD SCID mice. Mice were transferred i.v. with single purified T cell subsets.

Abbreviations: NOD, nonobese diabetic; SCID, severe combined immunodeficiency; MACS, magnetic bead-activated cell sorting; FACS, fluorescence-activated cell sorting.

§To whom correspondence should be addressed. E-mail: bach@necker.fr.

www.pnas.org/cgi/doi/10.1073/pnas.2636971100

Table 1. Histological analysis of pancreas, stomach, gut, thyroid, and salivary glands of NOD SCID mice reconstituted with distinct T cell subsets

T cell subset inoculum	Diabetes, %	Gastritis, %	Colitis, %	Thyroiditis, %	Sialitis, %
$CD25^-$ ($n = 56$)	71	95 (22m, 26M, 5S)	20 (4m, 7M)	30 (3m, 1M, 3S)	94 (29m, 19M)
$CD62L^-$ ($n = 7$)	100	0	0	ND	57 (3m, 1S)
$CD25^-CD62L^-$ ($n = 15$)	100	30 (5m)	0	0	67 (8m)
$CD25^-CD62L^+$ ($n = 38$)	8	90 (3m, 17M, 14S)	53 (15m, 5M)	10 (2m, 2M)	76 (19m, 10M)
$CD4^+CD45RB^{high}$ ($n = 8$)	0	12 (1m)	100 (1M, 7S, 2 ulceratives)	12 (1m)	37 (2m, 1S)
Total splenocytes ($n = 8$)	85	14 (1m)	0	0	14 (1m)
NOD mice (18-week-old) ($n = 30$)	80	0	66 (10m, 10M)	3 (1S)	66 (5m, 15M)
NOD SCID mice (10- to 18-week-old) ($n = 32$)	0	0	0	0	ND

For each organ, mononuclear infiltration was scored as minimal (m), moderate (M), or severe (S). ND, not done. Values in parentheses are absolute numbers of mice exhibiting each pattern.

For each experiment, cell numbers were expressed in terms of $CD4^+$ T cells, independently from the presence of B or $CD8^+$ T cells, which were deliberately not removed from the cell inoculum.

For cotransfer experiments, mice were injected either with just diabetogenic cells or with mixtures of diabetogenic and purified putative regulatory T cells.

Autoantibody Measurements. ***Antithyroglobulin antibodies.*** Autoantibodies were detected by solid-phase ELISA (11). Flat-bottom microtiter plates (Nunc, Life Technologies, Paisley, U.K.) were coated overnight at 4°C with porcine thyroglobulin (Sigma) (100 μg/ml in PBS). The plates were incubated for 2 h at room temperature with PBS containing 5% FCS. Fifty microliters of each serum sample was diluted 1/10 in PBS plus 5% FCS and incubated in duplicate for 2 h at room temperature. The plates were then incubated with a sufficient concentration of a horseradish peroxidase-labeled goat anti-mouse IgG antiserum (P.A.R.I.S., Compiègne, France). The enzymatic activity was revealed by using *O*-phenylenediamine dihydrochloride (Sigma) as a substrate. The reaction was stopped by 50 μl of 3 M HCl, and the optical density was evaluated at 490/650 nm.

Gastric anti-H^+/K^+ ATPase antibodies. Antibodies were detected by ELISA, as described (12). Porcine H^+/K^+ ATPase (α and β subunits) was purified by tomato–lectin affinity chromatography (13). Purity was assessed by SDS/PAGE and silver staining. Flat-bottom microtiter plates (Nunc) were coated overnight at 4°C with 100 μl of purified H^+/K^+ ATPase (0.5 μg/ml) in 50 mM carbonate–bicarbonate buffer, pH 9.6. Plates were then incubated for 2 h at 37°C with PBS plus FCS 5%. Fifty microliters of serum samples (diluted at 1/10 in PBS plus FCS 5%) was incubated for 2 h at room temperature. The plates were then incubated 1 h at room temperature with the adequate concentration of a streptavidin-biotinylated horseradish peroxidase-labeled goat anti-mouse IgG. The enzymatic activity was revealed as described.

Histopathology. Stomach, colon, pancreas, salivary glands, and thyroid were fixed in 4% formalin and processed according to standard methods. Five-micrometer-thick paraffin sections stained with hematoxylin/eosin–safran were examined. For each organ, mononuclear infiltration was scored as minimal, moderate, or severe.

For gastritis, inflammation was found around fundic glands, sometimes destroying the underlying glands leading to glandular atrophy. Neither epithelial dysplasia nor metaplasia was observed.

Colitis sometimes manifested as ulcerative colitis, with neutrophils infiltration, glandular atrophy, and necrosis.

***In Vitro* Proliferation Assays and Cytokine Production** For proliferation assays, cells were cultured in RPMI medium 1640 supplemented with glutamax/10% FCS/0.05 mM 2-mercaptoethanol/penicillin/streptomycin. Purified subsets using MACS or FACS were seeded in round-bottom 96-well microplates (0.2×10^5 cells of each subset per well), in a total volume of 200 μl per microwell. Cells were stimulated with purified soluble CD3 antibody (145 2C11, provided by Jeffrey A. Bluestone, University of California, San Francisco) (500 ng per microwell) in the presence of antigen-presenting cells (APCs) (1.25×10^5 mitomycin-treated APCs per well). Cells were cultured at 37°C for 72 h in a humidified atmosphere containing 5% CO_2 and pulsed with 1 μCi of [^{3}H]thymidine (2 μCi/mmol) (Amersham Pharmacia) for the last 18 h of culture. Then cells were harvested, and thymidine incorporation was assessed by using a Beta Plate scintillation counter (Perkin–Elmer). Data from the cocultures were expressed as the percent inhibition deduced as follows:

$$\% \text{ Inhibition} = [1 - (\text{cpm } (CD4^+CD25^- + CD4^+CD25^+)/\text{cpm } CD4^+CD25^-)] \times 100.$$

For cytokine production, lymphocytes were plated at 0.2×10^6 cells per well in a total volume of 200 μl per microwell and stimulated with immobilized CD3 antibody. Supernatants were recovered at 24, 48, and 72 h of culture and stored at −80°C until tested for IFNγ, IL-4, and IL-10.

IL-4 ELISA. Antibodies used were 11B11 (provided by W. Paul, National Institutes of Health, Bethesda) and biotinylated BVD6 (BD Pharmingen). Mouse recombinant IL-4, used as standard, was from R & D Systems. The sensitivity of the assay was 10 pg/ml.

IL-10 ELISA. Antibodies used were JES5-A5 (provided by A. O'Garra, DNAX) and biotinylated JES5-16E3 (BD Pharmingen). Mouse recombinant IL-10, used as standard, was from R & D Systems. The sensitivity of the assay was 10 pg/ml.

IFNγ ELISA. Antibodies used were R46A2 and biotinylated AN18 (provided by A. O'Garra). Mouse recombinant IFNγ, used as standard, was from R & D Systems. The sensitivity of the assay was 10 pg/ml.

Statistical Analysis. Diabetes incidence was plotted by using the Kaplan–Meier method, i.e., nonparametric cumulative survival plot. The statistical comparison between the curves was performed by using the log-rank (Mantel–Cox) test that provided the corresponding χ^2 values. Mean values were compared by using Student's t test.

Results

NOD and NOD SCID Mice Reconstituted with Syngeneic Total Spleen Cells Exhibit Overt Autoimmune Diabetes Concomitantly with Minor Gastritis and Colitis. In our colony, female NOD mice develop overt diabetes starting at 14–16 wk of age (95% incidence at 35 wk of age). At 18 wk of age, they also show, as already described, histological signs of thyroiditis and sialitis (14) (Table 1). Interestingly, they also exhibit histological manifestations typical of colitis (which, however, remain moderate and without wasting disease) but no gastritis (Table 1). No anti-H^+/K^+ ATPase or antithyroglobulin antibodies are detectable at this age.

Immunoincompetent NOD SCID mice reconstituted with total syngeneic spleen cells from prediabetic (10-wk-old) NOD mice

IMMUNOLOGY

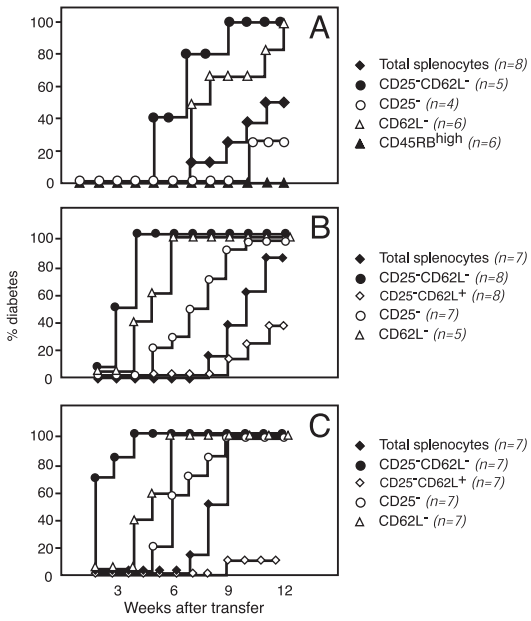

Fig. 1. Diversity of regulatory CD4$^+$ T cells controlling autoimmune diabetes. Results of a representative experiment show diabetes incidence in NOD SCID mice reconstituted with total spleen cells or spleen cells depleted in distinct regulatory T cell subsets from 10-wk-old NOD mice. Independent from the cell population analyzed, diabetes incidence correlated with the number of transferred cells, i.e., 1.25×10^6 (*A*), 4×10^6 (*B*), and 7×10^6 (*C*). The data highlight three main points. First, CD25$^-$CD62L$^-$ T cells are significantly more effective in transferring diabetes than total spleen cells [$P < 0.01$ (*A*), $P < 0.0002$ (*B*), and $P < 0.0001$ (*C*)]. Second, purified CD25$^-$CD62L$^-$ T cells triggered extremely severe diabetes at an incidence significantly higher than that observed in recipients of CD25$^-$CD62L$^+$ T cells [$P < 0.0001$ (*B*) and $P < 0.0001$ (*C*)]. Third, CD4$^+$CD45RB^{high} T cells that are very effective at transferring colitis were not diabetogenic at all.

exhibited overt diabetes at 7–8 wk posttransfer with kinetics that correlated with the number of transferred cells (Fig. 1). These adoptively transferred recipients also showed moderate histological signs of colitis (here again without overt wasting disease), together with histological sialitis and mild gastritis but not thyroiditis.

Unreconstituted 5- to 7-wk-old NOD SCID mice showed as their only histopathological manifestation a minor mononuclear cell infiltration of the colon that spontaneously disappeared with aging (Table 1 and Fig. 2).

The Main Candidate Regulatory T Cell Subset Phenotypes (CD25$^+$, CD62L$^+$, and CD45RB^{low}) Only Partially Overlap. CD4$^+$ T cells from 6- and 10-wk-old NOD mice were studied by flow cytometry for their expression of CD25, CD62L, and CD45RB. As shown in Table 2, there was only a modest correlation between these three phenotypic markers reported on CD4$^+$ regulatory T cells.

Thus, it was observed that both CD45RB^{low} and CD45RB^{high} T cells included a minority of CD25$^+$ T cells with a quasiabsence of CD25$^+$ T cells among CD45RB^{high} lymphocytes (Table 2). Similarly, CD62L$^+$ T cells included very low proportions of CD25$^+$ T cells (≈5%), only twice as many as the CD62L$^-$ T cell compartment (Table 2). Last, CD62L$^+$ T cells included a similar proportion of CD45RB^{low} T cells as compared to CD62L$^-$ T cells (≈40%) (data not shown).

Taken together, these results show that the regulatory T cell subsets defined by the CD25, CD62L, and CD45RB markers overlap only partially, suggesting that either these subsets are functionally distinct or that the relevant regulatory subset(s) represents only a minority of the cells composing the three populations defined by these markers.

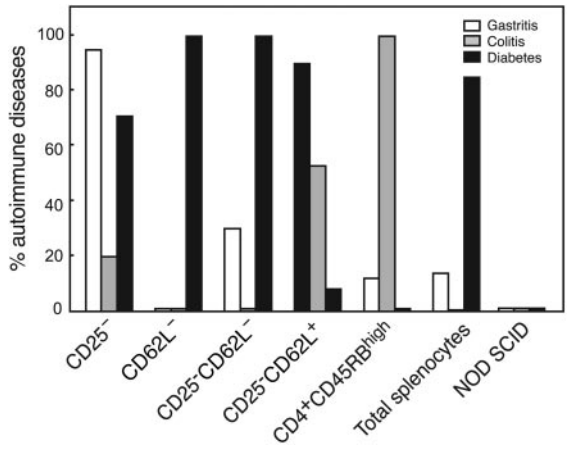

Fig. 2. Gastritis, colitis, and diabetes in NOD SCID mice reconstituted with spleen cells depleted of distinct regulatory T cell subsets. Incidence of overt diabetes and histological gastritis and colitis in a total of 194 NOD SCID mice reconstituted with various T cell subsets is shown. The major finding was that CD25$^-$CD62L$^+$, CD4$^+$CD45RB^{high}, and CD4$^+$CD62L$^-$ T cells were unique in their capacity to trigger almost exclusively one disease, namely gastritis, colitis, or diabetes, respectively. Intermediate patterns, both in terms of incidence and severity (see also Table 1), were observed for the other purified subsets.

Gastritis, Diabetes, and Colitis Are Selectively Induced on Adoptive Transfer of T Cells Depleted of Distinct Regulatory CD4$^+$ T Cell Subsets. Adoptive transfer experiments in NOD SCID recipients were performed by using CD4$^+$ T cells from 10-wk-old NOD females depleted in CD25$^+$, CD62L$^+$, or CD45RB^{low} regulatory T cells. In these various experimental conditions, recipients were monitored for the occurrence of various immune and autoimmune diseases, namely diabetes, gastritis, thyroiditis, sialitis, and colitis. The purified CD4$^+$ T cell subsets were supplemented with adequate proportions of purified B cells to allow the analysis of gastritis-specific anti-H$^+$/K$^+$ ATPase antibodies and of CD8$^+$ T cells, known to be mandatory for diabetes induction (15). Given the different kinetics of the various diseases analyzed when diabetes occurred, mice were treated with exogenous insulin to allow survival until 12 wk posttransfer, the time point at which the stomach, thyroid, salivary glands, and gut were recovered for histological examination.

Cells were purified by either MACS or FACS. For CD25$^+$- and CD62L$^+$-depleted populations, similar results were obtained by using the two methods. In the case of CD45RB^{low}-depleted cells, induction of overt disease with weight loss and wasting was obtained only by using FACS purification. MACS-purified T cells induced only histological colitis.

Table 2. Analysis of CD25, CD45RB, and CD62L expression by spleen CD4$^+$ T cells from 10-wk-old NOD mice

T cells	Percent CD62L$^+$ T cells	Percent CD62L$^-$ T cells	Percent CD25$^+$ T cells	Percent CD25$^-$ T cells
CD45RB^{high}	20–32	1–5	0–1	3–7
CD45RB^{low}	33–42	10–17	4–12	55–77
CD45RB$^-$	3–8	14–22	2–6	14–23
Total	61–75	25–38	6–14	85–94
	Percent CD62L$^+$ T cells	Percent CD62L$^-$ T cells		
CD25$^+$	2–6	0–2		
CD25$^-$	70–80	21–32		
Total	68–82	21–33		

Values shown for each given subset are expressed as the percentage of total CD4$^+$ T cells. For each subset, the range of values obtained from two to four independent experiments is presented.

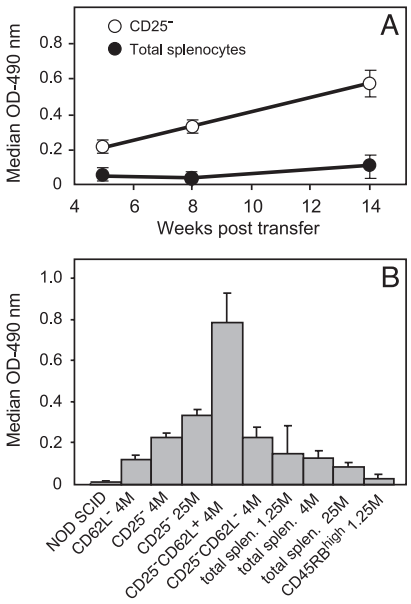

Fig. 3. Anti-H^+/K^+ ATPase autoantibody serum levels. Specific autoantibody levels were determined by ELISA. (*A*) Kinetics of anti-H^+/K^+ ATPase autoantibody production in mice reconstituted with 4×10^6 of either total spleen cells (●) or purified $CD25^-$ T cells (○). (*B*) Antibody levels at 12 wk posttransfer in the various groups of recipients analyzed. The *x* axis details the phenotype and the number (M, millions of cells) for each transferred lymphocyte subset. Mean antibody levels detected in recipients injected with $CD25^-CD62L^+$ T cells were significantly higher than those observed in all other groups ($P < 0.001$).

Gastritis is predominantly induced on adoptive transfer of $CD4^+CD25^+$-depleted T cells. As expected, diabetes was observed within 7–8 wk after transfer of $CD4^+CD25^+$-depleted T cells. The kinetics were similar to those observed in mice reconstituted with unseparated spleen cells (Fig. 1).

The results shown in Fig. 2 and Table 1 demonstrate that $CD25^+$ T cell depletion induced the onset of gastritis in 95% of recipients. This gastritis was associated with high serum levels of anti-H^+/K^+ ATPase autoantibodies, detectable as early as 6–7 wk after reconstitution (Fig. 3).

It is important to note that, unlike diabetes, the prevalence of both gastritis and anti-H^+/K^+ ATPase autoantibody levels was higher than that observed in NOD SCID mice reconstituted with unseparated spleen cells (Table 1 and Fig. 3).

Last, there was also evidence in these recipients of severe sialitis, mild thyroiditis (without detectable antithyroglobulin autoantibodies), and only moderate colitis (without wasting disease) (Table 1 and Fig. 2).

Diabetes is selectively induced on adoptive transfer of $CD4^+CD62L^+$-depleted T cells. NOD SCID mice reconstituted with $CD62L^-$ T cells showed an extremely rapid appearance of fulminant diabetes, leading to death within 8 days in the absence of insulin treatment. This pattern of diabetes was significantly different from that observed in NOD SCID mice reconstituted with unseparated cells for whom the disease appeared later and in a much less severe form (Fig. 1). In contrast, as observed in NOD SCID mice reconstituted with unseparated cells, recipients of $CD62L^+$-depleted T cells showed, on histological examination, sialitis, only moderate colitis (with no wasting disease), mild gastritis, and no thyroiditis (Table 1 and Fig. 2).

Similarly, in $CD62L^-$ T cell-reconstituted mice, antithyroglobulin and anti-H^+/K^+ ATPase antibodies were not found at higher frequency than in mice reconstituted with total spleen cells (Fig. 3).

Colitis is selectively induced on adoptive transfer of $CD4^+CD45RB^{low}$-depleted T cells. Injection of 0.5×10^6 of FACS-purified $CD4^+CD45RB^{high}$ spleen cells into NOD SCID recipients induced severe colitis with wasting disease (Fig. 2). As described by others in BALB/c recipients, mice started to develop cachexia as early as 5–6 wk after reconstitution. They were culled at 8 wk after transfer, when they already showed major weight loss (≥15%). At this stage, histological examination revealed no or minor gastritis or insulitis (Table 1). This latter observation is at variance with our previous report showing that immunoincompetent NOD mice restored with total $CD4^+$ T cells alone developed severe insulitis (16).

Experiments were performed in which $CD4^+CD45RB^{high}$ spleen cells were complemented with $CD8^+$ T cells and B cells. Despite the occurrence of colitis in these recipients, no diabetes was observed, although mice could be monitored up to 8 wk posttransfer, a time point when diabetes had already occurred in mice reconstituted with either $CD62L^-$ or $CD25^-$ T cells.

In addition, no anti-H^+/K^+ ATPase autoantibodies were observed in these same recipients, at a time point when NOD SCID mice reconstituted with $CD25^-$ T cells already showed significant autoantibody levels (Fig. 3).

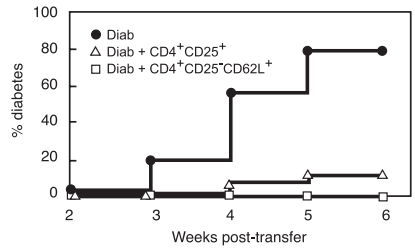

Fig. 4. Spleen $CD4^+CD25^+$ and $CD4^+CD25^-CD62L^+$ T cells from prediabetic NOD mice are protective *in vivo*. Diabetes was monitored in NOD SCID recipients injected with diabetogenic cells alone (Diab) or with mixtures of diabetogenic cells and 1×10^6 $CD4^+CD25^+$ or $CD4^+CD25^-CD62L^+$ purified T cells. In the two latter groups, significant diabetes protection was observed ($P < 0.0001$ for $CD4^+CD25^+$ and $CD4^+CD25^-CD62L^+$). Shown are combined data of six to seven independent experiments.

Direct Evidence for the Selective Protection from Gastritis and Diabetes Afforded by $CD25^+CD62L^-$ and $CD25^-CD62L^+$ T Cells. As previously mentioned, $CD25^-$ T cells ($CD25^+$-depleted) were effective in transferring both severe gastritis and mild diabetes. Moreover, $CD62L^-$ T cells ($CD62L^+$-depleted) triggered fulminant diabetes but no gastritis. We therefore wanted to explore whether combining the depletion of $CD25^+$ and $CD62L^+$ T cells would lead to the appearance of both severe gastritis and diabetes. Surprisingly, results showed that transfer of purified $CD25^-CD62L^-$ T cells induced extremely severe diabetes but no gastritis, suggesting that $CD25^-CD62L^+$ T cells have a positive influence on gastritis induction. We then analyzed in greater detail the disease-protecting ability of $CD25^-CD62L^+$ T cells.

As shown in Table 1 and Fig. 2, $CD25^-CD62L^+$ T cells induced only severe gastritis, with levels of anti-H^+/K^+ATPase autoantibodies significantly higher ($P < 0.001$) than those scored in the other groups (Fig. 3) but not diabetes. These results argue for the selective gastritis-protective capacity of $CD25^+CD62L^-$ T cells and the diabetes-protective capacity of $CD25^-CD62L^+$T cells. This latter conclusion was further supported by our cotransfer data.

Young NOD SCID recipients were injected i.v. with mixtures of two distinct populations, namely splenocytes from diabetic NOD mice (diabetogenic cells) and $CD25^+$ or $CD25^-CD62L^+$ T cells from the spleen of 6-wk-old prediabetic NOD mice. As shown in Fig. 4, as few as 1×10^6 purified $CD4^+CD25^+$ spleen T cells from prediabetic NOD mice significantly protected from diabetes transfer [$P < 0.0001$ as assessed by the log-rank test (Mantel–Cox)]. Interestingly, the $CD62L^+$ subset included within the $CD4^+CD25^-$ compartment also provided very efficient protection from diabetes transfer (Fig. 4).

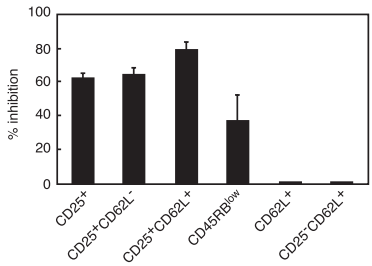

Fig. 5. *In vitro* suppression of $CD4^+CD25^-$ T cell proliferation by distinct regulatory T cell subsets. Data collected from different experiments are expressed as percent inhibition of proliferation. Results show that cells expressing the CD25 marker are the most effective suppressors *in vitro*. In great distinction, no suppression was exhibited by T cell subsets expressing CD62L but no CD25.

***In Vitro* Studies.** **In vitro *suppression*.** The capacity of the various T cell subsets discussed above to inhibit the proliferation of $CD25^-$ and of $CD25^-CD62L^-$ T cells was studied in a systematic fashion. As shown in Fig. 5, no inhibition was afforded by T cell subsets not expressing CD25. Thus, $CD62L^+CD25^-$ T cells did not suppress. Conversely, total $CD25^+$, $CD25^+CD62L^+$, and $CD25^+CD62L^-$ T cells significantly inhibited the proliferation of the responder population.

At variance with CD25, CD62L did not prove to be a good marker for *in vitro* suppressor cells because both $CD62L^+$ and $CD62L^-$ T cells proliferated and were not suppressive.

CD45RB expressed some capacity to discriminate between proliferative and suppressor cells because $CD45RB^{high}$ T cells proliferated more than $CD45RB^{low}$ T cells and $CD45RB^{low}$ T cells partially inhibited the proliferation of $CD45RB^{high}$ T cells (that included >99% $CD25^-$ T cells).

To ensure that total $CD62L^+$ T cells and $CD25^-CD62L^+$ T cells did not exhibit *in vitro* regulatory capacities, it was verified that carboxyfluorescein diacetate succinimidyl ester-labeled $CD25^-CD62L^-$ T cells underwent the same number of cell divisions when cultured alone or in the presence of $CD62L^+$ T cells or $CD25^-CD62L^+$ T cells (data not shown).

Cytokine production. The production of IFN-γ, IL-10, and IL-4 by the various cell subsets was analyzed after *in vitro* stimulation with CD3 antibody (Fig. 6). Although no absolute pattern was observed, clear-cut differences were noted in the cytokine pattern expressed by the various regulatory T cell subsets. Expression of CD25 was associated with low production of IFN-γ and IL-4 but with significant production of IL-10 whether $CD25^+CD62L^+$ or $CD25^+CD62L^-$ T cells were taken into consideration. $CD4^+CD25^-$ T cells produced significantly larger amounts of IFN-γ and significantly lower amounts of IL-10 than $CD4^+CD25^+$ T cells ($P < 0.0001$ and $P < 0.015$, respectively). IFN-γ was secreted in higher amounts by $CD4^+CD62L^-$ T cells than by $CD4^+CD62L^+$ T cells. Production of IL-4 and IL-10 was quasiabsent in $CD62L^+$ T cells but quite high in the $CD62L^-$ population. Removal of $CD25^+$ T cells from the $CD62L^-$ population ($CD25^-CD62L^-$) did not modify IFN-γ and IL-4 production but slightly decreased that of IL-10. Conversely, removal of $CD25^+$ T cells from the $CD62L^+$ population ($CD25^-CD62L^+$) had no effect on the production of the three cytokines. Last, both $CD45RB^{low}$ and $CD45RB^{high}$ T cells produced extremely low amounts of IFN-γ, IL-10, and IL-4.

Interestingly, when $CD25^-CD62L^-$ T cells were injected into NOD SCID mice, the T cells recovered from the diabetic recipient mice showed a cytokine pattern different from that of the initial cell inoculum. In brief, IFN-γ production remained high, whereas IL-4 and IL-10 production was dramatically reduced (data not shown).

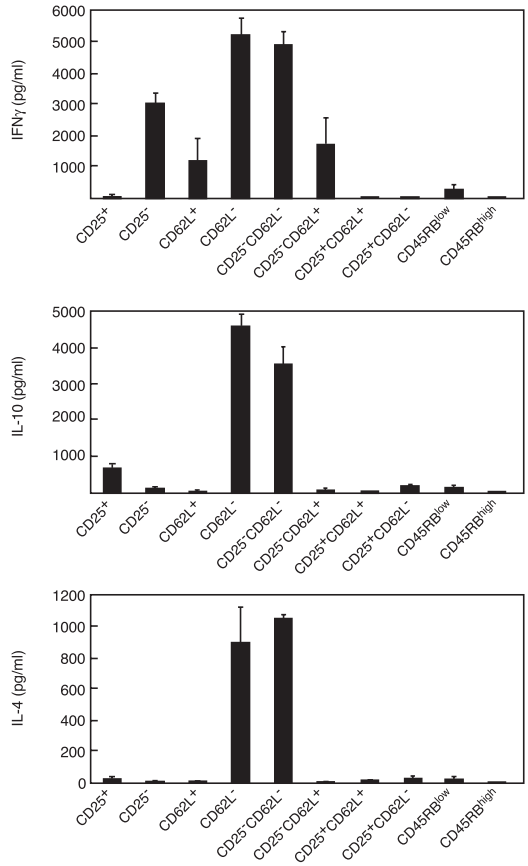

Fig. 6. Cytokine production by selected T cell subsets after CD3 antibody-induced stimulation. Results show that the cytokine-producing ability greatly differed among the distinct subsets analyzed. Mean values observed with $CD62L^-$ and $CD25^-CD62L^-$ T cells were significantly higher for the three cytokines analyzed than those observed for all other T cell subsets tested ($P < 0.0001$).

Discussion

There is compelling evidence to show that depletion of one or several candidate regulatory T cell subsets ($CD45RB^{low}$, $CD25^+$, and $CD62L^+$) induces distinct clinical manifestations such as colitis, autoimmune gastritis, or diabetes (1, 2). There is a questionable trend supporting the notion that a single population of regulatory T cells, predominantly $CD25^+$, is involved in the control of these three immune diseases (3, 17, 18). Differences in results obtained after mouse reconstitution with $CD25^-$ or $CD45RB^{high}$ T cells have been explained by the variety of the experimental conditions used (thymectomy, SCID vs. nude mice). To address this issue, we studied a model in which the three immune diseases could be induced by using a single mouse strain (NOD), in a given lymphopenic condition (NOD SCID), thus avoiding biases due to variable experimental conditions. Importantly, the colony of mice used in the present study harbored intestinal bacteria necessary for the induction of colitis, as assessed by the presence of both histological signs of mild colitis in wild-type NOD mice and by the development of severe colitis and wasting disease after reconstitution of NOD SCID mice with purified $CD45RB^{high}$ T cells.

We demonstrate here that $CD25^+$ T cells are essential in controlling the onset of gastritis, whereas $CD45RB^{low}$ are indispensable for the control of colitis. Moreover, $CD62L^+$ T cells play the key role in controlling diabetes with $CD25^+$ T cells also participating, albeit to a lesser extent.

It was important to ensure that, in the adoptive transfer experiments, all lymphocyte subsets necessary for the induction of the immune disorders in question (B cells, $CD4^+$, and $CD8^+$ T cells) were present in the cell inoculum. Gastritis can be induced with purified $CD4^+CD25^-$ T cells and does not require B cells if the read-out is limited to the infiltration of the stomach, but production

of antigastric autoantibodies (anti-H^+/K^+ ATPase) requires the presence of B cells (data not shown). Colitis leading to wasting disease is observed solely through the transfer of purified $CD4^+CD45RB^{high}$ T cells (4). Last, transfer of autoimmune diabetes, a T cell-mediated disease, requires the concomitant presence of $CD4^+$ and $CD8^+$ T cells when polyclonal diabetogenic T cells are used (15), even though, when islet-specific monoclonal T cells are used, disease transfer can be obtained solely by $CD4^+$ or $CD8^+$ lymphocytes (19, 20). In the present study, to allow a fair comparison of the three diseases (gastritis, colitis, and diabetes), the cell inocula were adapted to include the relevant cell populations (B cells for antigastric antibodies and $CD8^+$ T cells for diabetes). The age of the cell donors was also carefully selected (10 wk) to ensure the presence of pathogenic cells for each model (21). Finally, the recipients were monitored for a sufficient time to allow each disease to develop. Thus, when diabetes occurred, mice were treated with insulin to allow survival for sufficient time to monitor for gastritis and colitis.

Another approach for dissecting regulatory T cells controlling autoimmunity consists of studying their capacity to inhibit CD3-specific antibody-induced T cell proliferation. For this purpose, we studied the capacity of each of the regulatory subsets just mentioned to suppress in coculture the proliferation of $CD4^+CD25^-$ T cells (22, 23). In addition, we examined the cytokine pattern of each of the T cell subsets in question.

Taken together, the *in vivo* and *in vitro* data obtained in this study indicated that $CD25^+$ T cells exhibit the unique capacity to protect from gastritis *in vivo* and to inhibit the CD3 antibody-induced proliferation of $CD25^-$ T cells. $CD62L^+$ T cells have a very selective ability to protect from diabetes *in vivo*, and $CD45RB^{low}$ T cells possess the unique ability to protect from colitis *in vivo*.

Among the possible mechanisms explaining these differences, one may first suggest variable homing capacities of the relevant regulatory T cells possibly relying on a differential expression of chemokine receptors. This is in keeping with the recent data showing that $CD25^+CD62L^+$ T cells that protect from diabetes in NOD mice selectively express CCR7 (18). In the same vein, one might consider differences in chemokine receptor expression on effector T cells. Other homing receptors could be involved, such as L-selectin, discussed in this paper. However, one should mention that $CD62L^{-/-}$ NOD mice do not exhibit accelerated diabetes onset (24).

Another hypothesis relates to the differential cytokine dependency of each autoimmune disorder. $CD45RB^{low}$ T cell control of colitis is IL-10- and TGF-β-dependent (25, 26). Diabetes protection in NOD mice is TGF-β-dependent (L.C., unpublished results) but IL-4- and IL-10-independent (7). Gastritis protection by $CD25^+$ T cells has not been shown to depend on any cytokine, suggesting the possible requirement of direct cell–cell contact (1). One may postulate that $CD25^+$, $CD62L^+$, and $CD45RB^{low}$ T cells produce different cytokine patterns, either systemically or locally in the target organ, that in turn influence the organ specificity of the immune disorder they control. Our data are in keeping with such interpretation. $CD25^+$ T cells exhibit a high IL-10:IFN-γ ratio compared to $CD25^-$ T cells. $CD62L^+$ T cells produce hardly detectable levels of IL-4 and IL-10 but significant amounts of IFN-γ. In contrast, $CD62L^-$ T cells produce large amounts of the three cytokines. Although these data support the notion of a differential pattern of cytokine expression by individual regulatory T cell subsets, they do not fully correlate with the *in vivo* cytokine dependency just mentioned. The data may be reconciled by the fact that cytokine patterns may change after *in vivo* transfer, as exemplified by our observation with $CD25^-CD62L^-$ T cells, which before transfer produced high amounts of IL-4 and IL-10 *in vitro* that significantly decreased after *in vivo* parking.

Last, we mention the possibility of different mechanisms for triggering immunoregulation according to the cellular subset. The autoantigen-specific triggering of $CD25^+$ regulatory T cells has been suggested (1, 2), whereas autoantigen specificity has not been demonstrated for colitis, which involves antibacterial responses (8, 9). Moreover, in colitis, a role for homeostatic competition has been suggested. Thus, increasing the number of $CD45RB^{high}$ T cells did not provoke a more severe colitis but rather a significant decrease of its incidence (27), at variance with what was observed for transferred $CD25^-$ T cells, where the higher the number, the worse the disease (28). One may hypothesize that $CD45RB^{low}$ T cells are particularly good competitors for homeostatic signals (such as IL-7 and MHC peptide recognition), whereas $CD25^+$ T cells act essentially through antigen-specific mechanisms.

In conclusion, these data indicate that three of the main candidate regulatory T cell subsets show major differences in their functional activities both *in vivo* and *in vitro*. Each population appears to control a different immune disorder in a predominant fashion. *In vitro* suppression is essentially a property of $CD25^+$ T cells, with no obvious role for $CD62L^+$ T cells and a dubious one for $CD45RB^{low}$ T cells. These results militate against a unitary view of regulatory T cells. They also pose the problem of the general significance of *in vitro* suppression in coculture and of the differences in the mechanisms involved in controlling the various immune disorders under study.

We are indebted to Fabrice Valette and Michael Garcia for managing the animal facility, to Meriam Belghith for assistance with cotransfer experiments, to Berta Segovia for important technical help, to Martine Netter for iconography, and to Jérôme Mégret for assistance with FACS. We also thank J. A. Bluestone, W. Paul, and A. O'Garra for providing the monoclonal antibodies used in the study. This work was supported by grants from the Institut National de la Santé et de la Recherche Médicale, the Association Claude Bernard, and the Juvenile Diabetes Research Foundation.

1. Shevach, E. M. (2002) *Nat. Rev. Immunol.* **2,** 389–400.
2. Bach, J. F. (2003) *Nat. Rev. Immunol.* **3,** 189–198.
3. Asano, M., Toda, M., Sakaguchi, N. & Sakaguchi, S. (1996) *J. Exp. Med.* **184,** 387–396.
4. Powrie, F., Leach, M. W., Mauze, S., Caddle, L. B. & Coffman, R. L. (1993) *Int. Immunol.* **5,** 1461–1471.
5. Herbelin, A., Gombert, J. M., Lepault, F., Bach, J. F. & Chatenoud, L. (1998) *J. Immunol.* **161,** 2620–2628.
6. Lepault, F., Gagnerault, M. C., Faveeuw, C., Bazin, H. & Boitard, C. (1995) *Eur. J. Immunol.* **25,** 1502–1507.
7. Lepault, F. & Gagnerault, M. C. (2000) *J. Immunol.* **164,** 240–247.
8. Hudcovic, T., Stepankova, R., Cebra, J. & Tlaskalova-Hogenova, H. (2001) *Folia Microbiol. (Praha)* **46,** 565–572.
9. Rath, H. C., Schultz, M., Freitag, R., Dieleman, L. A., Li, F., Linde, H. J., Scholmerich, J. & Sartor, R. B. (2001) *Infect. Immun.* **69,** 2277–2285.
10. Gombert, J. M., Herbelin, A., Tancrede-Bohin, E., Dy, M., Carnaud, C. & Bach, J. F. (1996) *Eur. J. Immunol.* **26,** 2989–2998.
11. Tang, H., Mignon-Godefroy, K., Meroni, P. L., Garotta, G., Charreire, J. & Nicoletti, F. (1993) *Eur. J. Immunol.* **23,** 275–278.
12. Chuang, J. S., Callaghan, J. M., Gleeson, P. A. & Toh, B. H. (1992) *Autoimmunity* **12,** 1–7.
13. Callaghan, J. M., Toh, B. H., Simpson, R. J., Baldwin, G. S. & Gleeson, P. A. (1992) *Biochem. J.* **283**, 63–68.
14. Bach, J. F. (1994) *Endocr. Rev.* **15,** 516–542.
15. Bendelac, A., Carnaud, C., Boitard, C. & Bach, J. F. (1987) *J. Exp. Med.* **166,** 823–832.
16. Thivolet, C., Bendelac, A., Bedossa, P., Bach, J. F. & Carnaud, C. (1991) *J. Immunol.* **146,** 85–88.
17. Read, S., Malmstrom, V. & Powrie, F. (2000) *J. Exp. Med.* **192,** 295–302.
18. Szanya, V., Ermann, J., Taylor, C., Holness, C. & Fathman, C. G. (2002) *J. Immunol.* **169,** 2461–2465.
19. Haskins, K., Portas, M., Bergman, B., Lafferty, K. & Bradley, B. (1989) *Proc. Natl. Acad. Sci. USA* **86,** 8000–8004.
20. Wong, F. S., Visintin, I., Wen, L., Flavell, R. A. & Janeway, C. A., Jr. (1996) *J. Exp. Med.* **183,** 67–76.
21. Kuniyasu, Y., Takahashi, T., Itoh, M., Shimizu, J., Toda, G. & Sakaguchi, S. (2000) *Int. Immunol.* **12,** 1145–1155.
22. Thornton, A. M. & Shevach, E. M. (1998) *J. Exp. Med.* **188,** 287–296.
23. Takahashi, T., Kuniyasu, Y., Toda, M., Sakaguchi, N., Itoh, M., Iwata, M., Shimizu, J. & Sakaguchi, S. (1998) *Int. Immunol.* **10,** 1969–1980.
24. Friedline, R. H., Wong, C. P., Steeber, D. A., Tedder, T. F. & Tisch, R. (2002) *J. Immunol.* **168,** 2659–2666.
25. Asseman, C., Mauze, S., Leach, M. W., Coffman, R. L. & Powrie, F. (1999) *J. Exp. Med.* **190,** 995–1004.
26. Powrie, F., Carlino, J., Leach, M. W., Mauze, S. & Coffman, R. L. (1996) *J. Exp. Med.* **183,** 2669–2674.
27. Barthlott, T., Kassiotis, G. & Stockinger, B. (2003) *J. Exp. Med.* **197,** 451–460.
28. Sakaguchi, S., Sakaguchi, N., Asano, M., Itoh, M. & Toda, M. (1995) *J. Immunol.* **155,** 1151–1164.